



Cite this: *Soft Matter*, 2025, 21, 6791

A splay-twist phase stabilized by the interaction between the nematic and torsional fields in nematics

I. Lelidis, *^a G. Barbero ^{bc} and L. R. Evangelista ^{cde}

A free energy density for the nematic phase with two symmetry elements – the director, \mathbf{n} , and the vector defining the helix direction, \mathbf{t} – can be constructed as an extension of the Frank free energy. This formulation has already proven effective in demonstrating that the phase transition between the conventional nematic phase and the twist-bend nematic phase is of second order, characterized by a finite wave vector. In this work, we theoretically investigate the possibility that new periodic phases with finite wave vectors may be energetically favored over uniform structures within the framework of this elastic model. We show that splay-twist-like periodic structures naturally emerge from this theoretical approach. Furthermore, we demonstrate that the existence of a critical wave vector, which determines the periodicity of the non-uniform structure, depends on the elastic parameters, the sample thickness, and the anchoring energy strengths. A key role is played by the elastic constant that couples the nematic director to the helical axis: a distinctive feature of these materials. The splay-twist transition from the uniform nematic phase occurs only when the magnitude of the coupling elastic constant exceeds a threshold value. In this study, we specifically treat the case of a sample with symmetrical interfaces.

Received 31st May 2025,
Accepted 19th July 2025

DOI: 10.1039/d5sm00565e

rsc.li/soft-matter-journal

I. Introduction

Heliconical phases can arise in chiral nematic (cholesteric) or smectic liquid crystals, particularly in the presence of strong flexoelectric effects, applied electric fields, or specific molecular architectures (e.g., bent-core or dimeric molecules).^{1–7} They are important in soft matter physics, with potential applications in tunable photonic devices, bistable displays, and responsive materials. The twist-bend nematic (N_{TB}) phase is a well-known example of such a self-assembled heliconical phase, observed in bent-core and dimeric liquid crystal molecules. Exploring the possibility of splay-twist or splay-bend phases in this context is particularly interesting because these phases could arise from similar mechanisms of spontaneous symmetry breaking in nonchiral systems.

Since the experimental discovery of the twist-bend nematic (TBN) phase,^{8–10} extensive research has been conducted in the

field of modulated nematic phases. The properties of the TBN phase have been thoroughly investigated both experimentally^{11–20} and theoretically.^{21–36} Numerous theoretical approaches have been proposed,^{21–25,33–36} and a variety of models are available for describing the TBN phase as well as other modulated nematic and smectic phases.^{37,38}

Ten years ago, we proposed a generalization of the Frank elastic energy for conventional nematics^{39–41} to account for modulated nematic phases, in particular the twist-bend nematic phase.²⁵ This model is based on the introduction of a torsion field that couples to the nematic director field, enabling the emergence of modulated phases in a nematic medium composed of achiral mesogenic molecules.

More recently, using the same elastic theory framework, we demonstrated that tuning the elastic constant governing the coupling between the nematic and torsion fields can destabilize the uniform nematic phase with respect to one-dimensional (1D) deformations of the director, which may be either periodic or evanescent.⁴² In the present work, adopting the same approach as in ref. 42, we investigate whether fluctuations of the nematic director can destabilize the uniform phase and promote the formation of a two-dimensional (2D) modulated splay-twist nematic (STN) phase.

Our study is organized as follows. Section II briefly recalls the free energy density introduced in ref. 25. Section III presents the perturbation method, derives the second-order

^a Department of Condensed Matter Physics, Faculty of Physics, National and Kapodistrian University of Athens, Panepistimiopolis, Zografos, Athens 157 84, Greece. E-mail: ilelidis@phys.uoa.gr

^b Department of Applied Science and Technology, Politecnico di Torino, Corso Duca degli Abruzzi 24, 10129 Torino, Italy

^c Istituto dei Sistemi Complessi (ISC-CNR), Via dei Taurini, 19, 00185 Rome, Italy

^d Departamento de Física, Universidade Estadual de Maringá Avenida Colombo, 5790-87020-900 Maringá, Paraná, Brazil

^e Department of Molecular Science and Nanosystems, Ca'Foscari University of Venice, Via Torino 155, 30175 Mestre (VE), Italy



approximation of the free energy density, and formulates the corresponding equilibrium equations. In Section IV, the problem is solved for a symmetric sample. Section V presents the quadratic form of the free energy. In Section VI, a stability analysis of the energy is carried out. In particular, the critical value of the coupling constant is determined, along with the dependence of the instability wavevector on this coupling. Finally, Section VII is devoted to concluding remarks and future perspectives.

II. Elastic energy density of modulated phases

Frank elastic energy of a nematic^{39–41} was extended in ref. 25 to include the case of modulated nematic phases composed of achiral molecules. To this end, in addition to the nematic director field \mathbf{n} , a torsion field, represented by a unit vector \mathbf{t} , was introduced. It was argued that the nematic elastic energy density can then be expressed, up to second order, in the following form:

$$\begin{aligned} f = & f_0 - \frac{1}{2}\eta(\mathbf{n} \cdot \mathbf{t})^2 + \kappa_1(\mathbf{n} \cdot \mathbf{t})(\nabla \cdot \mathbf{n}) + \kappa_2 \mathbf{n} \cdot (\nabla \times \mathbf{n}) \\ & + \kappa_3 \mathbf{t} \cdot [\mathbf{n} \times (\nabla \times \mathbf{n})] + \frac{1}{2}K_{11}(\nabla \cdot \mathbf{n})^2 \\ & + \frac{1}{2}K_{22}[\mathbf{n} \cdot (\nabla \times \mathbf{n})]^2 + \frac{1}{2}K_{33}(\mathbf{n} \times \nabla \times \mathbf{n})^2 \\ & - (K_{22} + K_{24})\nabla \cdot (\mathbf{n}\nabla \cdot \mathbf{n} + \mathbf{n} \times \nabla \times \mathbf{n}) \\ & + \mu_1[\mathbf{t} \cdot (\mathbf{n} \times \nabla \times \mathbf{n})]^2 + \nu_1[\mathbf{t} \cdot \nabla(\mathbf{t} \cdot \mathbf{n})]^2 \\ & + \nu_2[\mathbf{t} \cdot \nabla(\mathbf{n} \cdot \mathbf{t})(\nabla \cdot \mathbf{n})] + \nu_3[\nabla(\mathbf{t} \cdot \mathbf{n})]^2 \\ & + \nu_4[(\mathbf{t} \cdot \nabla)\mathbf{n}]^2 + \nu_5[\nabla(\mathbf{n} \cdot \mathbf{t}) \cdot (\mathbf{t} \cdot \nabla)\mathbf{n}] \\ & + \nu_6 \nabla(\mathbf{n} \cdot \mathbf{t}) \cdot (\nabla \times \mathbf{n}). \end{aligned} \quad (1)$$

The usual Frank expression for the free energy density^{39–41} can be recovered if we put $\mathbf{t} = 0$ in eqn (1), as can be easily verified. In this perspective, the present energy density may be regarded as a generalization of the Frank energy that can be used as a theoretical framework to describe the orientational properties of those actual and potential stable phases of liquid-crystalline systems characterized by the elements of symmetry \mathbf{t} and \mathbf{n} .

III. Perturbation & equilibrium equations

To investigate the stability of a uniform planar orientation against small nematic fluctuations, we consider a slab-shaped sample of thickness d . Following the approach of ref. 42, we introduce a Cartesian coordinate system where the x -axis defines the planar easy axis, and the z -axis is perpendicular to the confining surfaces, located at $z = -d/2$ and $z = d/2$. The basis unit vectors \mathbf{e}_i , with $i = x, y, z$, represent the Cartesian

directions. The uniform nematic orientation under analysis is given by $\mathbf{n}_0 = \mathbf{e}_x$.

Small perturbations of the nematic director are described by the fluctuation vector $\mathbf{u} = u_x \mathbf{e}_x + u_y \mathbf{e}_y + u_z \mathbf{e}_z$, such that the perturbed director is expressed as $\mathbf{n} = \mathbf{n}_0 + \mathbf{u}$. Since we are concerned with infinitesimal deviations from the planar orientation, the components u_i are considered small quantities. The normalization condition $|\mathbf{n}| = 1$ then imposes the constraint

$$u_x \approx -\frac{1}{2}(u_y^2 + u_z^2). \quad (2)$$

Consequently, u_x is a second-order quantity in terms of the director variations.

Additionally, we assume that our “generalized” nematic state is characterized by $\mathbf{t} = \mathbf{e}_x$. The surface treatment enforces an easy axis along \mathbf{e}_x as discussed in ref. 42. Within the Rapini–Papoular approximation, the surface energy is given by $f_s = -(w/2)(\mathbf{n} \cdot \mathbf{e}_x)^2$. Expanding this expression up to second order and using eqn (2), we obtain

$$f_s = -\frac{w}{2} + \frac{w}{2}(u_y^2 + u_z^2), \quad (3)$$

where w denotes the anchoring energy strength of both surfaces. That is, we restrict our investigation to the case of two surfaces with identical anchoring direction and energy, $w_1 = w_2 = w$, which we call symmetric boundary conditions (BCs). These symmetric BCs also assume that splay and twist deformations have the same anchoring energy.

In the problem we are analyzing here $u_y = u_y(y, z)$ and $u_z = u_z(y, z)$, *i.e.*, the perturbation lies in a plane normal to the bounding surfaces. The energy density is given by

$$\begin{aligned} f(u_i, u_{i,j}) = & f_0 - \frac{1}{2}\eta + \frac{1}{2}\eta(u_y^2 + u_z^2) \\ & + \kappa_2(u_{z,y} - u_{y,z}) + \kappa_1(u_{y,y} + u_{z,z}) \\ & + \frac{1}{2}K_{11}(u_{y,y} + u_{z,z})^2 + \frac{1}{2}K_{22}(u_{z,y} - u_{y,z})^2 \\ & - 2(K_{22} + K_{24})(u_{y,y}u_{z,z} - u_{y,z}u_{z,y}), \end{aligned} \quad (4)$$

in which $u_{i,j} = \partial u_i / \partial x_j$. Finally, the total energy per unit length is

$$\mathcal{F} = \int_{\mathcal{D}} f(u_i, u_{i,j}) dy dz + \int_{\gamma} f_s ds \quad (5)$$

where \mathcal{D} is the surface of the sample perpendicular to the x -axis, and γ is its border. Hereafter, summation convention on repeated indices is assumed when appropriate. The first variation of \mathcal{F} is

$$\begin{aligned} \delta \mathcal{F} = & \int_{\mathcal{D}} \left\{ \frac{\partial f}{\partial u_i} - \frac{\partial}{\partial x_j} \left(\frac{\partial f}{\partial u_{i,j}} \right) \right\} \delta u_i dy dz \\ & + \int_{\gamma} \left(\nu_j \frac{\partial f}{\partial u_{i,j}} + \frac{\partial f_s}{\partial u_i} \right) \delta u_i ds. \end{aligned} \quad (6)$$

where ν_j denotes the outwards geometrical normal characterizing the surface while $x_1 = x$, $x_2 = y$, $x_3 = z$. The functions minimizing eqn (5) are solutions of the partial differential



equations⁴³

$$\frac{\partial f}{\partial u_i} - \frac{\partial}{\partial x_j} \left(\frac{\partial f}{\partial u_{i,j}} \right) = 0, \quad (7)$$

for all points in \mathcal{D} , and on γ satisfy the following boundary condition:

$$\nu_j \frac{\partial f}{\partial u_{i,j}} + \frac{\partial f_s}{\partial u_i} = 0. \quad (8)$$

In the following we are interested in the possibility of periodic deformation along y - z plane. In this case \mathcal{D} is the domain limited by a rectangle of sides λ and d , and γ its contour, where λ is the periodicity of the deformation to be determined. For simplicity, we rewrite the fundamental equations above in an explicit form as follows. For $i = y, z$, as we consider here, eqn (7) become

$$\begin{aligned} \frac{\partial f}{\partial u_y} - \frac{\partial}{\partial y} \left[\frac{\partial f}{\partial u_{y,y}} \right] - \frac{\partial}{\partial z} \left[\frac{\partial f}{\partial u_{y,z}} \right] &= 0, \\ \frac{\partial f}{\partial u_z} - \frac{\partial}{\partial y} \left[\frac{\partial f}{\partial u_{z,y}} \right] - \frac{\partial}{\partial z} \left[\frac{\partial f}{\partial u_{z,z}} \right] &= 0. \end{aligned} \quad (9)$$

Likewise, the BCs, eqn (8), become

$$\pm \frac{\partial f}{\partial u_{y,z}} + \frac{\partial f_s}{\partial u_y} = 0 \quad \text{and} \quad \pm \frac{\partial f}{\partial u_{z,z}} + \frac{\partial f_s}{\partial u_z} = 0, \quad (10)$$

at $z = -d/2$ (−) and $z = d/2$ (+).

Taking into account the free energy density, eqn (4), the partial differential equations for $u_y(y, z)$ and $u_z(y, z)$, stated in eqn (9), are found to be

$$K_{11}u_{y,yy} + K_{22}u_{y,zz} + (K_{11} - K_{22})u_{z,zy} - \eta u_y = 0, \quad (11)$$

$$K_{22}u_{z,yy} + K_{11}u_{z,zz} + (K_{11} - K_{22})u_{y,yz} - \eta u_z = 0. \quad (12)$$

These equations have to be solved with the BCs expressed via eqn (10), which simply read

$$\pm \{-\kappa_2 + K_{22}u_{y,z} + (K_{22} + 2K_{24})u_{z,y}\} + wu_y = 0, \quad (13)$$

$$\pm \{\kappa_1 + K_{11}u_{z,z} + [K_{11} - 2(K_{22}K_{24})]u_{y,y}\} + wu_z = 0. \quad (14)$$

IV. Modulated solutions

We look for solutions of the type

$$u_i(y, z) = L_i(z) + M_i(y, z), \quad (15)$$

where, as before, $i = y, z$. Substituting the ansatz (15) into eqn (11) and (12) we deduce that $L_i(z)$ are solutions of the ordinary differential equations:

$$K_{22}L_y'' - \eta L_y = 0, \quad (16)$$

$$K_{11}L_z'' - \eta L_z = 0, \quad (17)$$

whereas $M_i(y, z)$ are solutions of the partial differential equations

$$K_{11}M_{y,yy} + K_{22}M_{y,zz} + (K_{11} - K_{22})M_{z,zy} - \eta M_y = 0, \quad (18)$$

$$K_{22}M_{z,yy} + K_{11}M_{z,zz} + (K_{11} - K_{22})M_{y,yz} - \eta M_z = 0. \quad (19)$$

In this framework, they have to be solved using the BCs

$$\pm \left(-\kappa_2 + K_{22}L_y' \right) + wL_y = 0, \quad (20)$$

$$\pm \left(\kappa_1 + K_{11}L_z' \right) + wL_z = 0, \quad (21)$$

and

$$\pm \{K_{22}M_{y,z} + (K_{22} + 2K_{24})M_{z,y}\} + wM_y = 0, \quad (22)$$

$$\pm \{K_{11}M_{z,z} + [K_{11} - 2(K_{22} + K_{24})]M_{y,y}\} + wM_z = 0, \quad (23)$$

respectively. The components $L_y(z)$ and $L_z(z)$ of the ansatz correspond to the case where the fluctuations components depend only on z . This case corresponds to a 1D deformation of the director field, which can be periodic or not, and has been analyzed in ref. 42. Hereafter, we investigate the possibility of periodic 2D solutions $M_i(y, z)$, $i = y, z$, that satisfy the homogeneous bulk differential equations and BCs. To accomplish this task, we seek solutions of the form

$$M_y(y, z) = G(z)\sin(qy) \quad \text{and} \quad M_z(y, z) = F(z)\cos(qy), \quad (24)$$

where $q = 2\pi/\lambda$.⁴⁴ Note that for $q = 0$, $M_y(y, z) = 0$ and $M_z(y, z) = F(z)$, i.e. we recover the case of 1D deformation treated in ref. 42.

Substituting eqn (24) into eqn (18) and (19), we get

$$K_{22}G''(z) - (\eta + q^2K_{11})G(z) - q(K_{11} - K_{22})F'(z) = 0, \quad (25)$$

$$K_{11}F''(z) - (\eta + q^2K_{22})F(z) + q(K_{11} - K_{22})G'(z) = 0, \quad (26)$$

for $-d/2 \leq z \leq d/2$, to be solved using the BCs

$$\pm \{K_{22}G' - q(K_{22} + 2K_{24})F\} + wG = 0, \quad (27)$$

$$\pm \{K_{11}F' + q[K_{11} - 2(K_{22} + K_{24})]G\} + wF = 0. \quad (28)$$

Eqn (25) and (26) form a system of linear ordinary differential equations with constant coefficients, to be solved with the BCs eqn (27) and (28) that are also linear with constant coefficients; therefore the solutions are of exponential form. In addition, from the structure of these equations, it follows that each of the functions $F(z)$ and $G(z)$ must be either symmetric or antisymmetric with respect to z , with the additional constraint that if $G(z)$ is even, then $F(z)$ must be odd, and *vice versa*. For definiteness, we have chosen to consider this case in what follows. Therefore, for a cell with identical interfaces, the solutions of the linear system defined by eqn (25) and (26) take the form

$$G(z) = A_1 \cosh(\mu_1 z) + A_3 \cosh(\mu_3 z), \quad (29)$$

$$F(z) = B_1 \sinh(\mu_1 z) + B_3 \sinh(\mu_3 z).$$

A_1, A_2, B_1, B_3 are integration constants, and μ_1, μ_3 are two parameters to be determined. Substituting eqn (29) into eqn (25) and (26) yields a homogeneous system of two equations, which admits a non-trivial solution only if

$B_k = R_k A_k$, where

$$R_1 = -\frac{\mu_1}{q} \quad \text{and} \quad R_3 = -\frac{q}{\mu_3}. \quad (30)$$

μ_1 and μ_3 are defined using the following expressions:

$$\mu_1 = \sqrt{q^2 + \frac{\eta}{K_{11}}} \quad \text{and} \quad \mu_3 = \sqrt{q^2 + \frac{\eta}{K_{22}}}. \quad (31)$$

The set of BCs, eqn (27) and (28), reduces to

$$\{K_{22}G'(d/2) - q(K_{22} + 2K_{24})F(d/2)\} + wG(d/2) = 0, \quad (32)$$

$$\{K_{11}F'(d/2) + q[K_{11} - 2(K_{22} + K_{24})]G(d/2)\} + wF(d/2) = 0, \quad (33)$$

These BCs, using the solutions eqn (29), may be put in the matrix form as follows:

$$\begin{bmatrix} a_{11} & a_{13} \\ a_{31} & a_{33} \end{bmatrix} \cdot \begin{bmatrix} A_1 \\ A_3 \end{bmatrix} = 0, \quad (34)$$

in which

$$\begin{aligned} a_{11} &= w \cosh\left(\mu_1 \frac{d}{2}\right) + [-(K_{22} + 2K_{24})qR_1 + K_{22}\mu_1] \sinh\left(\mu_1 \frac{d}{2}\right), \\ a_{13} &= w \cosh\left(\mu_3 \frac{d}{2}\right) + [-(K_{22} + 2K_{24})qR_3 + K_{22}\mu_3] \sinh\left(\mu_3 \frac{d}{2}\right), \\ a_{31} &= wR_1 \sinh\left(\mu_1 \frac{d}{2}\right) \\ &\quad + [-2(K_{22} + K_{24})q + K_{11}(q + R_1\mu_1)] \cosh\left(\mu_1 \frac{d}{2}\right), \\ a_{33} &= wR_3 \sinh\left(\mu_3 \frac{d}{2}\right) \\ &\quad + [-2(K_{22} + K_{24})q + K_{11}(q + R_3\mu_3)] \cosh\left(\mu_3 \frac{d}{2}\right). \end{aligned} \quad (35)$$

Thus, nontrivial solutions can be obtained by imposing that

$$P = \det \begin{bmatrix} a_{11} & a_{13} \\ a_{31} & a_{33} \end{bmatrix} = 0, \quad (36)$$

Solving eqn (36) implies handling a nonlinear transcendental equation of the form:

$$q_c = f(q_c, d, w, K_{11}, K_{22}, K_{24}, \eta), \quad (37)$$

thus exploring many possibilities in a parameter space formed by four elastic constants, the thickness of the sample, and the anchoring strength.⁴⁴ Once a physically meaningful solution is obtained for eqn (37), we have to analyze the sign of the corresponding quadratic form representing the excess free energy density promoted by the nonuniform structure represented by $M_i(y, z)$, for $i = y, z$.

V. The quadratic form of energy

In the preceding section, we obtained the analytical profile of the nematic director fluctuations.

$$\begin{aligned} u_y(y, z) &= L_y(z) + G(z) \sin(qy), \\ u_z(y, z) &= L_z(z) + F(z) \cos(qy), \end{aligned} \quad (38)$$

where $G(z)$, $F(z)$ are given by eqn (29). Substituting these expressions into eqn (4), the free energy density separates in three contributions:

$$f = f_{1D} + f_c + f_{2D}, \quad (39)$$

where the free energy of the uniform planar state (the ground state) was taken to be zero. f_{1D} refers to the 1D-deformation, specifically the $L_y(z)$, $L_z(z)$ components of the solutions, and its expression is given in ref. 42. f_c includes coupling terms between the $L_i(z)$ and $M_i(y, z)$ solutions, while f_{2D} refers to the 2D-deformations.

Averaging the bulk free energy density over a period $\lambda = 2\pi/q$ and considering only 2D deformations yields

$$\begin{aligned} f_{2D}(z) &= \frac{1}{4}\eta[G(z)^2 + F(z)^2] + \frac{1}{4}K_{11}[qG(z) + F'(z)]^2 \\ &\quad + \frac{1}{4}K_{22}[qF(z) + G'(z)]^2 \\ &\quad - (K_{22} + K_{24})q[G(z)F'(z) + F(z)G'(z)]. \end{aligned} \quad (40)$$

The bulk energy is calculated by integration of the latter equation along the z -direction. Likewise, the surface part of the free energy density, after averaging over y may be written as follows:

$$f_s = \frac{1}{4}w[F(d/2)^2 + F(-d/2)^2 + G(d/2)^2 + G(-d/2)^2]. \quad (41)$$

Finally, the total energy of the system is expressed as a quadratic form:

$$\mathcal{F} = \frac{1}{2} \sum_{k=1}^2 \sum_{l=1}^2 M_{kl} A_k A_l, \quad (42)$$

in which the elements of the matrix \mathbf{M} are formally given by

$$M_{ij} = \frac{\partial^2 \mathcal{F}}{\partial A_i \partial A_j}. \quad (43)$$

To analyze the stability of the solutions, one must examine the signs of the principal minors of the matrix \mathbf{M} . The uniform state is stable as long as these minors have positive determinants, namely $M_1 = M_{11}$ and $M_2 = M_{11}M_{22} - M_{12}M_{21}$. If at least one of them become negative, the uniform state can no longer be considered stable.⁴⁵ In such a case, the system may instead favor a non-uniform structure which, in the scenario under analysis, corresponds to a periodic structure characterized by a small but nonzero wave vector q .



VI. Stability analysis

Hereafter, we examine the stability of the solutions, considering the cases $\eta = 0$ and $\eta \neq 0$ separately.

1. $\eta = 0$

First, we treat the case of the absence of elastic coupling between the two fields. In the special case for $\eta = 0$, $\mu_1 = \mu_3 = q$, $R_1 = R_3 = -1$, the elements a_{ij} are given by

$$\begin{aligned} a_{11} = a_{13} &= w \cosh\left(q\frac{d}{2}\right) + 2(K_{24} + K_{22})q \sinh\left(q\frac{d}{2}\right), \\ a_{33} = a_{31} &= -w \sinh\left(q\frac{d}{2}\right) - 2(K_{22} + K_{24})q \cosh\left(q\frac{d}{2}\right), \end{aligned} \quad (44)$$

and therefore $P = 0$ identically. The total energy per unit length, in the case under consideration, is given by

$$\mathcal{F} = \frac{1}{2}(A_1 + A_3)^2 [w \cosh(qd) + 2(K_{22} + K_{24})q \sinh(qd)],$$

from which it follows that the minimum of \mathcal{F} is reached for $A_1 + A_3 = 0$, *i.e.* for a non-deformed state.

2. $\eta \neq 0$

Before proceeding to the general case $\eta \neq 0$, it is convenient to define the reduced wavevector $q_r = q/q_0$ and the reduced coupling elastic constant $\eta_r = \eta/\eta_0$, where we introduced a reference wavevector $q_0 = \pi/d$ and a reference coupling constant $\eta_0 = K_{11}q_0^2$. In Fig. 1, the left panel shows the first principal

minor determinant M_1 , while the right panel shows $M_2 = \det[\mathbf{M}]$ as a function of q_r , for four representative values of η_r/η_c , where η_c is the critical value of $\eta < 0$ below which periodic solutions emerge. The curves in Fig. 1 were calculated using the following parameter set: $K_{11} = 5 \times 10^{-11}$ N, $K_{22} = K_{11}/5$, $K_{24} = 0.9K_{22}$,^{14,35} $d = 10$ μm and $w = 2 \times 10^{-5}$ J m⁻². It is observed that M_1 remains positive for all values of η_r . However, M_2 becomes negative when $\eta_r/\eta_c > 1$. Notably, for $\eta > 0$, M_2 remains positive, indicating that the 2D-perturbations of the splay-twist nematic phase are suppressed. Solving numerically the equation $M_2 = 0$, we find that the critical value of the coupling constant is $\eta_c = -0.165491\eta_0$. The analysis of this case is particularly insightful, as it permits an analytical treatment that sheds light on the role of various parameters in the emergence of non-uniform periodic structures, as discussed in the following sections.

In general, M_2 may have more than one zero. However, due to the harmonic approximation used in the energy expansion, only the longest wavelength mode of the instability is retained. By solving the equation $M_2 = 0$ numerically, we obtained the two dotted curves shown in Fig. 2, which represent the variation of q_r as a function of η_r . Both solutions intersect the horizontal axis ($q = 0$) at finite values of the coupling constant, denoted η_{c_1} and $\eta_{c_2} < \eta_{c_1}$. However, only the rightmost curve fulfills the condition $P = 0$ that allows a non-trivial solutions for A_i , and hence a deformed state as discussed above, eqn (36). Therefore, the critical value of the coupling constant is given by $\eta_{c_1} = \eta_c$. In the same figure, the solution to the condition $P = 0$ is shown as

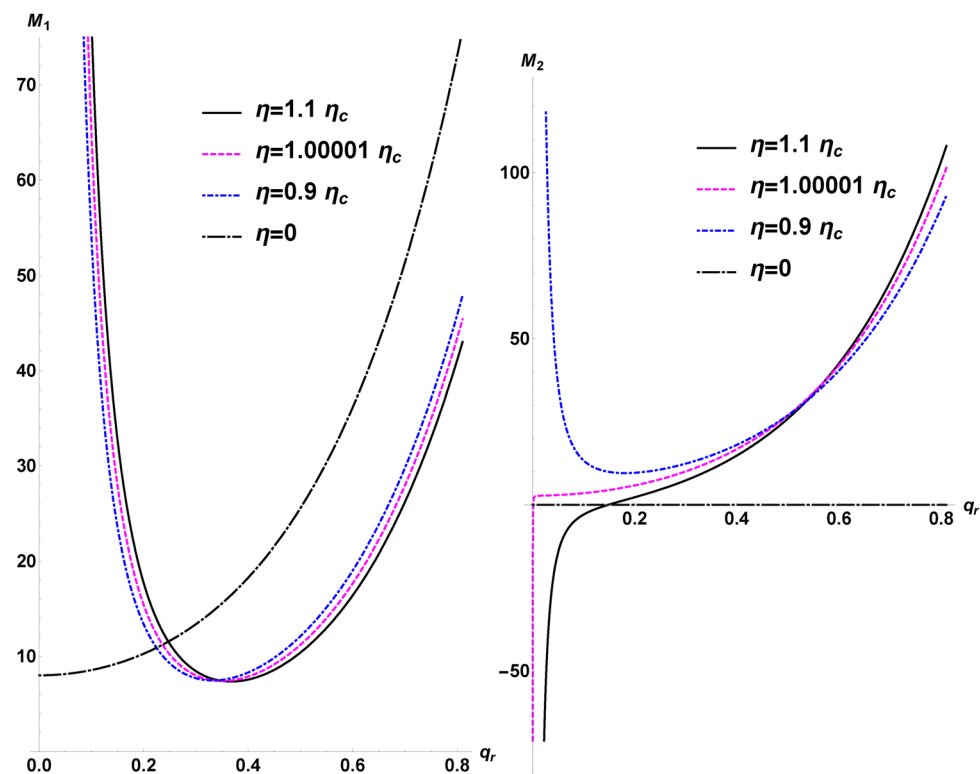


Fig. 1 M_1 left panel and M_2 right panel, versus the reduced wavevector $q_r = q/q_0$ for a few representative values of η as shown in the graph. For $\eta/\eta_c > 1$, M_2 change sign while $M_1 > 0$, and the uniform nematic phase is destabilized.



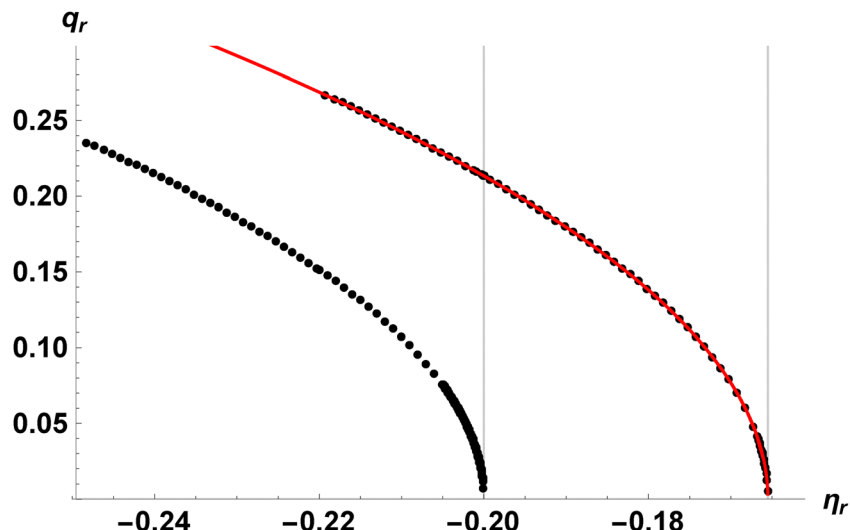


Fig. 2 The reduced wave-vector q_r of the instability versus η_r . The black solid points are calculated from the condition $M_2 = 0$. The red line is calculated from $P = 0$. The vertical line at $\eta_r = -0.165491$ corresponds to the minimal value, $|\eta_c|$ given by eqn (52). Numerical values are as in previous simulations. For $q_r \rightarrow 0$, η_r goes to its critical value η_c which is the weakest value of $|\eta_r|$ where the uniform nematic destabilizes. The second vertical line at $\eta_r = -0.2$ would correspond to another branch of instability.

the red continuous line. The asymptotes at η_c and η_{c_2} also indicated in the figure, are calculated in the next section.

$$n_1(\eta_r) = K_{11}q_0\sqrt{\eta_r} \cosh\left(\frac{\pi}{2}\sqrt{\eta_r}\right) + w \sinh\left(\frac{\pi}{2}\sqrt{\eta_r}\right), \quad (47)$$

3. P expansion for $q \rightarrow 0$

The critical value η_c of η for $q \rightarrow 0$ can be evaluated from eqn (36). In the limit $q \rightarrow 0$, expanding P in power series of q , we get

$$P = \alpha(\eta) \frac{n_1(\eta)n_2(\eta)}{q} + m(\eta)q, \quad (45)$$

where

$$\alpha(\eta_r) = \sqrt{\eta_r}, \quad (46)$$

For the set of elastic parameters considered in our analysis, $m(\eta_r)$ takes negative values approximately in the range $-1 < \eta_r < 0$, as shown in Fig. 3.

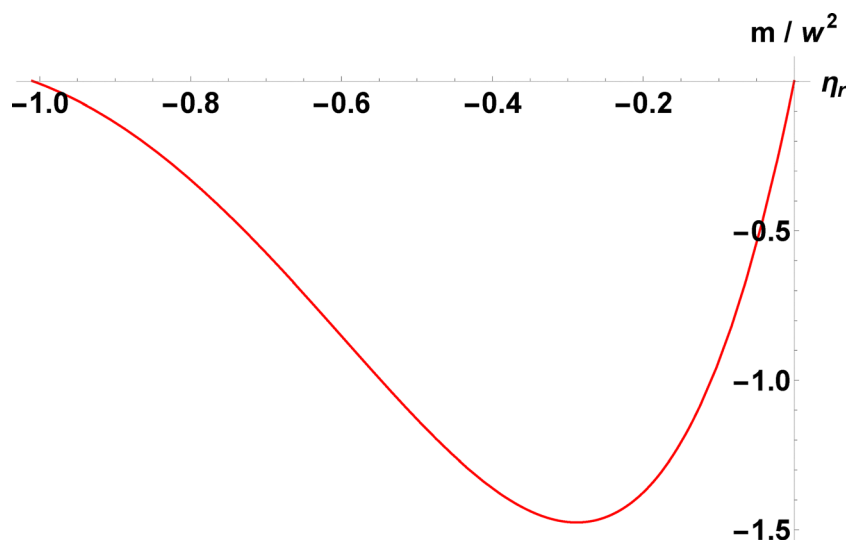


Fig. 3 Function $m = m(\eta_r)$ in the range $-1.009 \leq \eta_r \leq 0$. m is plotted in units of w^2 .



The condition $P = 0$ gives

$$q_r = \sqrt{-\alpha(\eta_r) \frac{n_1(\eta_r) n_2(\eta_r)}{m(\eta_r)}}. \quad (49)$$

From (49), taking into account eqn (46)–(48), it follows that q is a real quantity for $n_2(\eta_r) \leq 0$, vanishing for $n_2(\eta_c) = 0$, *i.e.*, for

$$w \cosh\left(\frac{\pi}{2}\sqrt{\frac{K_{11}}{K_{22}}}\eta_c\right) + q_0 \sqrt{K_{11}K_{22}\eta_c} \sinh\left(\frac{\pi}{2}\sqrt{\frac{K_{11}}{K_{22}}}\eta_c\right) = 0. \quad (50)$$

Fig. 2 shows two branches of the numerical solutions of eqn (50). Modulated solutions appear only for $\eta_r < \eta_c$. In addition, a second threshold appears at a smaller value of η_r . Other branches also may appear at even lower values of η_r as can be calculated from eqn (50). Rearranging the latter equation we get the equation for η_c as follows:

$$\frac{dw}{\pi K_{22}} = -\sqrt{\frac{K_{11}}{K_{22}}}\eta_c \tanh\left(\frac{\pi}{2}\sqrt{\frac{K_{11}}{K_{22}}}\eta_c\right). \quad (51)$$

Since the instability takes place for $\eta_c < 0$, eqn (51) can be rewritten as

$$\frac{dw}{\pi K_{22}} = \sqrt{\frac{K_{11}}{K_{22}}|\eta_c|} \tan\left(\frac{\pi}{2}\sqrt{\frac{K_{11}}{K_{22}}|\eta_c|}\right). \quad (52)$$

Eqn (52) is of some importance for this analysis since it allows the investigation of the dependence of η_c on the anchoring energy w and the thickness d of the sample. The first two thresholds for η_r are depicted by the vertical asymptote lines in Fig. 2.

Returning to the numerical analysis, we observe that it is straightforward to track the evolution of this zero as a function of q_r . Indeed, Fig. 4 shows a typical plot of $\delta = wd/K_{22}$ vs. η_c obtained from the roots of the equation $M_2 = 0$, represented by solid points, which were calculated numerically by solving eqn (36). The continuous line in Fig. 4 represents the approximate

solution given by eqn (52), in the limit $q \rightarrow 0$. Note that as $\eta_c \rightarrow 0$ the anchoring energy $w \rightarrow 0$ as well. Writing δ as $\delta = d/L_{22}$, we conclude that $|\eta_c|$ increases as the twist extrapolation length of the interfaces, L_{22} , becomes shorter, that is, for stronger anchoring as expected.

The above analysis shows that, for a given liquid crystalline material characterized by a set of elastic constants K_{11} , K_{22} , K_{24} and η , the uniform nematic phase becomes unstable when the magnitude of η exceeds a critical value η_c . For a given material, this critical coupling elastic constant, η_c , depends on the sample thickness and on the anchoring energy. In other words, confinement and surface effects can suppress splay-twist fluctuations.

The transition from the uniform nematic state to the splay-twist nematic phase can be described within the framework of Landau–de Gennes theory as a second order phase transition, with the modulation wavevector q serving as the order parameter. The corresponding free energy density of the STN phase can be expressed as follows:

$$f_{st} = f_u + \frac{1}{2}a(\eta - \eta_c)q^2 + \frac{1}{4}bq^4 + \dots \quad (53)$$

where the elastic coupling, η , between the two fields plays the role of the temperature, while a , b are positive phenomenological parameters, and f_u denotes the free energy density of the uniform nematic phase. Minimization of the free energy yields $q = \pm\sqrt{-a(\eta - \eta_c)/b}$. By fitting the curve $q_r(\eta_r)$ shown in Fig. 2, with a function of the form $q = [-a(\eta - \eta_c)/b]^\beta$, one finds $\beta = 0.50$ and $a/b = 1.31$.

Finally, it is important to clarify that there is no competition between the splay-twist and twist-bend modulations. It is now well established that the bend elastic constant K_{33} remains positive¹⁸ even in the vicinity of the twist-bend phase. According to our previous work²⁵ which analyzed the emergence of the twist-bend phase, it was shown that for $K_{33} > 0$, this phase appears for positive values of the elastic constant η above a critical value η_{TB} , that is, $\eta > \eta_{TB} > 0$. In contrast, the splay-

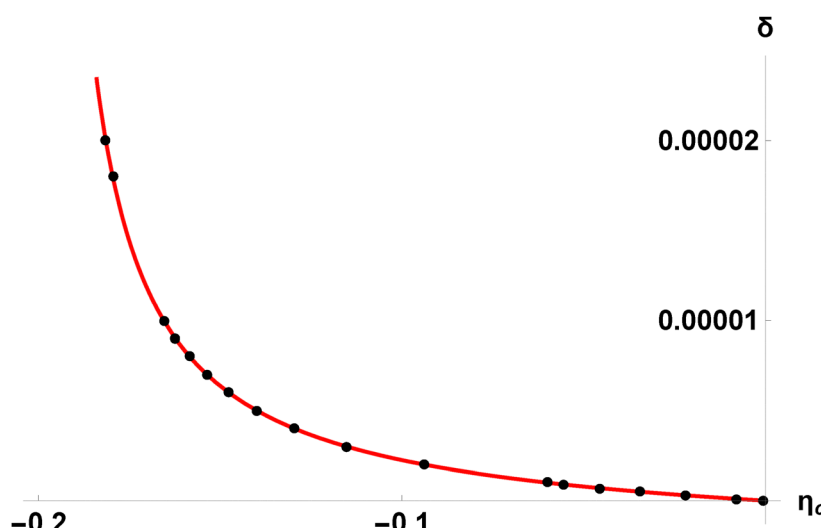


Fig. 4 Dependence of the reduced anchoring energy $\delta = wd/K_{22}$ as a function of η_r , for a fixed value of the instability wavevector $q_r = 10^{-5}$. Solid points are numerical solutions of $M_2 = 0$ while the continuous line is calculated analytically from the approximated solution eqn (52).



twist periodic deformation predicted in the present work occurs only for $\eta < \eta_c < 0$, and therefore does not interfere with the twist-bend phase.

VII. Concluding remarks

We explored the possibility that a nonuniform equilibrium configuration could be energetically favored in a context involving heliconical liquid crystals.

To this end, we started from an elastic energy density proposed as an extension of the Frank free energy for liquid-crystalline media, in which there are essentially two fundamental symmetry elements: the director, \mathbf{n} , a hallmark of conventional liquid crystals, and the helix director, \mathbf{t} , which appears to be crucial for the existence of periodic structures in systems composed of bent-core or dimer molecules. This same free energy expression, which we proposed in recent years, has already proven capable of describing the emergence and stability of a periodic structure characteristic of the experimentally observed twist-bend phase.²⁵

Our analysis follows a simple yet thermodynamically rigorous approach to investigating this possibility.⁴⁴ We assumed the existence of a uniform planar-like structure in the medium described by this elastic model and explored the possibility that a nonuniform structure could arise due to fluctuations of the director in the plane perpendicular to this uniform configuration. The general equations of the problem were analytically established for a slab-shaped sample of thickness d , characterized by the presence of a finite anchoring energy (weak anchoring) and the absence of an external field.

Within this system, everything behaves as if this new symmetry element, represented by the helix director \mathbf{t} , acts as a (intrinsic) field and plays a crucial role in the emergence of these new structures. A periodic solution ansatz was proposed, and we were able to demonstrate that it can be energetically favored in the liquid-crystalline medium depending on the values of the elastic parameters, the sample thickness, and the anchoring energy. This occurs because the periodic solutions satisfy boundary conditions such that a wave vector q assumes realistic critical values as a function of the other macroscopic parameters characterizing the sample, in the form of a transcendental equation of the type $q = f(q, d, w, K_{11}, K_{22}, K_{24})$.

In fact, a numerical analysis of the involved solutions reveals the real possibility that a splay-twist-like phase is inherently present in the free energy density expression we proposed and may soon be experimentally observed.

To achieve this result, we fixed the values of the anchoring energy, the sample thickness, and the other elastic parameters, except for the parameter η , a new elastic constant that acts as the coupling strength between the director and the helix direction. We demonstrated how this parameter plays a crucial role in the emergence of a critical wave vector associated with the favored periodicity in the system, *i.e.*, the periodic structure that modifies the sign of the quadratic form in a linearized elastic model, causing it to transition from positive definiteness

– corresponding to the uniform planar structure – to an energy regime where the minors of the matrix representing the quadratic form become negative.

A more comprehensive analysis, which would make the present work excessively long but could be developed as a complementary study, should explore a broader range of elastic parameter values, particularly those of the sample thickness and the anchoring energy. Moreover, the general case of a non-symmetric cell could be of interest, that is, a cell where anchoring energy is different for the two interfaces and/or the twist and splay anchoring energies are unequal.

This should be addressed in future work, as the study of the emergence of such structures as a function of surface properties may be important not only for the liquid-crystalline systems considered here but also, more broadly, for many finite-size systems in condensed matter physics.

Conflicts of interest

There are no conflicts to declare.

Data availability

This manuscript is theoretical in nature and does not involve the use or generation of any data.

References

- 1 R. B. Meyer, Effects of electric and magnetic fields on the structure of cholesteric liquid crystals, *Appl. Phys. Lett.*, 1968, **12**, 281–282, DOI: [10.1063/1.1651992](https://doi.org/10.1063/1.1651992).
- 2 R. D. Kamien, Liquids with Chiral Bond Order, *J. Phys. II*, 1996, **6**, 461–475.
- 3 V. L. Lorman and B. Mettout, Unconventional Mesophases Formed by Condensed Vector Waves in a Medium of Achiral Molecules, *Phys. Rev. Lett.*, 1999, **82**, 940, DOI: [10.1103/PhysRevLett.82.940](https://doi.org/10.1103/PhysRevLett.82.940).
- 4 I. Dozov, On the spontaneous symmetry breaking in the mesophases of achiral banana-shaped molecules, *Europhys. Lett.*, 2001, **56**, 247, DOI: [10.1209/epl/i2001-00513-x](https://doi.org/10.1209/epl/i2001-00513-x).
- 5 R. Memmer, Liquid crystal phases of achiral banana-shaped molecules: a computer simulation study, *Liq. Cryst.*, 2002, **29**, 483, DOI: [10.1080/02678290110104586](https://doi.org/10.1080/02678290110104586).
- 6 T. C. Lubensky and L. Radzhovsky, Theory of bent-core liquid-crystal phases and phase transitions, *Phys. Rev. E: Stat., Nonlinear, Soft Matter Phys.*, 2002, **6**, 031704, DOI: [10.1103/PhysRevE.66.031704](https://doi.org/10.1103/PhysRevE.66.031704).
- 7 A. Jákli, O. D. Lavrentovich and J. V. Selinger, Physics of liquid crystals of bent-shaped molecules, *Rev. Mod. Phys.*, 2018, **90**, 045004(68), DOI: [10.1103/RevModPhys.90.045004](https://doi.org/10.1103/RevModPhys.90.045004).
- 8 V. P. Panov, M. Nagaraj, J. K. Vij, Yu. P. Panarin, A. Kohlmeier, M. G. Tamba, R. A. Lewis and G. H. Mehl, Spontaneous periodic deformations in nonchiral planar-aligned bimesogens with a nematic-nematic transition



and a negative elastic constant, *Phys. Rev. Lett.*, 2010, **105**, 167801, DOI: [10.1103/PhysRevLett.105.167801](https://doi.org/10.1103/PhysRevLett.105.167801).

9 M. Cestari, S. Diez-Berart, D. A. Dunmur, A. Ferrarini, M. R. de la Fuente, D. J. B. Jackson, D. O. Lopez, G. R. Luckhurst, M. A. Perez-Jubindo, R. M. Richardson, J. Salud, B. A. Timimi and H. Zimmermann, Phase behavior and properties of the liquid-crystal dimer 1",7"-bis(4-cyanobiphenyl-4'-yl) heptane: A twist-bend nematic liquid crystal, *Phys. Rev. E: Stat., Nonlinear, Soft Matter Phys.*, 2011, **84**, 031704, DOI: [10.1103/PhysRevE.84.031704](https://doi.org/10.1103/PhysRevE.84.031704).

10 V. Borshch, Y.-K. Kim, J. Xiang, M. Gao, A. Jákli, V. P. Panov, J. K. Vij, C. T. Imrie, M. G. Tamba, G. H. Mehl and O. D. Lavrentovich, Nematic twist-bend phase with nano-scale modulation of molecular orientation, *Nat. Commun.*, 2013, **4**, 2635, DOI: [10.1038/ncomms3635](https://doi.org/10.1038/ncomms3635).

11 D. Chen, M. Nakata and R. Shao, *et al.*, Twist-bend heliconical chiral nematic liquid crystal phase of an achiral rigid bent-core mesogen, *Phys. Rev. E: Stat., Nonlinear, Soft Matter Phys.*, 2014, **89**, 022506, DOI: [10.1103/PhysRevE.89.022506](https://doi.org/10.1103/PhysRevE.89.022506).

12 Y. Wang, G. Singh and D. M. Agra-Kooijman, *et al.*, Room temperature heliconical twist-bend nematic liquid crystal, *CrystEngComm*, 2015, **17**, 2778, DOI: [10.1039/C4CE02502D](https://doi.org/10.1039/C4CE02502D).

13 K. Adlem, M. Čopić and G. R. Luckhurst, *et al.*, Chemically induced twist-bend nematic liquid crystals, liquid crystal dimers, and negative elastic constants, *Phys. Rev. E: Stat., Nonlinear, Soft Matter Phys.*, 2013, **88**, 022503, DOI: [10.1103/PhysRevE.88.022503](https://doi.org/10.1103/PhysRevE.88.022503).

14 C. J. Yun, M. R. Vengatesan and K. Jagdish, *et al.*, Hierarchical elasticity of bimesogenic liquid crystals with twist-bend nematic phase, *Appl. Phys. Lett.*, 2015, **106**, 173102, DOI: [10.1063/1.491906](https://doi.org/10.1063/1.491906).

15 B. Robles-Hernandez, N. Sebastian and M. Rosario de la Fuente, *et al.*, Twist, tilt, and orientational order at the nematic to twist-bend nematic phase transition of 1",9"-bis(4-cyanobiphenyl-4'-yl) nonane: A dielectric, 2H NMR, and calorimetric study, *Phys. Rev. E: Stat., Nonlinear, Soft Matter Phys.*, 2015, **92**, 062505, DOI: [10.1103/PhysRevE.92.062505](https://doi.org/10.1103/PhysRevE.92.062505).

16 G. Babakhanova, Z. Parsouzi and S. Paladugu, *et al.*, Elastic and viscous properties of the nematic dimer CB7CB, *Phys. Rev. E*, 2017, **96**, 062704, DOI: [10.1103/PhysRevE.96.062704](https://doi.org/10.1103/PhysRevE.96.062704).

17 J. Sellarès, J. A. Diego and D. O. López, *et al.*, Comparative dielectric and thermally stimulated-depolarization-current studies of the liquid crystal dimers 1",9"-bis(4-cyanobiphenyl-4'-yl) nonane and heptane and a binary mixture between them, close to the glass transition, *Phys. Rev. E*, 2022, **106**, 054702, DOI: [10.1103/PhysRevE.106.054702](https://doi.org/10.1103/PhysRevE.106.054702).

18 A. Jákli, Y. Nastishin and O. D. Lavrentovich, Defects in bent-core liquid crystals, *Liq. Cryst. Rev.*, 2023, **11**, 48–73, DOI: [10.1080/21680396.2022.2086932](https://doi.org/10.1080/21680396.2022.2086932).

19 C. Yuan, Y. Zhan and H. Liu, *et al.*, Room temperature stable twist-bend nematic materials without crystallization over 1 year, *Giant*, 2024, **19**, 100290.

20 S. B. Atata, G. Basina and V. Tzitzios, *et al.*, Influence of chalcopyrite nanoplatelets on nematic phases of bend-shaped dimeric molecules: Phase diagram, birefringence, and reorientation transition, *J. Mol. Liq.*, 2024, **412**, 125842, DOI: [10.3390/nano13222980](https://doi.org/10.3390/nano13222980).

21 C. Greco and A. Ferrarini, Entropy-Driven Chiral Order in a System of Achiral Bent Particles, *Phys. Rev. Lett.*, 2015, **115**, 147801, DOI: [10.1103/PhysRevLett.115.147801](https://doi.org/10.1103/PhysRevLett.115.147801).

22 S. M. Shamid, S. Dhakal and J. V. Selinger, Statistical mechanics of bend flexoelectricity and the twist-bend phase in bent-core liquid crystals, *Phys. Rev. E: Stat., Nonlinear, Soft Matter Phys.*, 2013, **87**, 052503, DOI: [10.1103/PhysRevE.87.052503](https://doi.org/10.1103/PhysRevE.87.052503).

23 S. M. Shamid, D. W. Allender and J. V. Selinger, Predicting a Polar Analog of Chiral Blue Phases in Liquid Crystals, *Phys. Rev. Lett.*, 2014, **113**, 237801, DOI: [10.1103/PhysRevLett.113.237801](https://doi.org/10.1103/PhysRevLett.113.237801).

24 E. Virga, Double-well elastic theory for twist-bend nematic phases, *Phys. Rev. E: Stat., Nonlinear, Soft Matter Phys.*, 2014, **89**, 052502, DOI: [10.1103/PhysRevE.89.052502](https://doi.org/10.1103/PhysRevE.89.052502).

25 G. Barbero, L. R. Evangelista and M. P. Rossetto, *et al.*, Elastic continuum theory: Towards understanding of the twist-bend nematic phases, *Phys. Rev. E: Stat., Nonlinear, Soft Matter Phys.*, 2015, **92**, 030501(R), DOI: [10.1103/PhysRevE.92.030501](https://doi.org/10.1103/PhysRevE.92.030501).

26 R. S. Zola, G. Barbero and I. Lelidis, *et al.*, A continuum description for cholesteric and nematic twist-bend phases based on symmetry considerations, *Liq. Cryst.*, 2017, **44**, 24–30, DOI: [10.1080/02678292.2016.1229054](https://doi.org/10.1080/02678292.2016.1229054).

27 R. S. Zola, R. R. Ribeiro de Almeida and G. Barbero, *et al.*, Behaviour of twist-bend nematic structure under a uniform magnetic field, *Mol. Cryst. Liq. Cryst.*, 2017, **649**, 71–78, DOI: [10.1080/02678292.2016.1229054](https://doi.org/10.1080/02678292.2016.1229054).

28 M. P. Rossetto, R. R. Ribeiro de Almeida and R. S. Zola, *et al.*, Nanometric pitch in modulated structures of twist-bend nematic liquid crystals, *J. Mol. Liq.*, 2019, **267**, 266–270, DOI: [10.1016/j.molliq.2018.01.050](https://doi.org/10.1016/j.molliq.2018.01.050).

29 I. Lelidis I and E. Kume, A new flexoelectric mode in twist-bend nematic liquid crystals, *J. Mol. Liq.*, 2019, **295**, 111707, DOI: [10.1016/j.molliq.2019.111707](https://doi.org/10.1016/j.molliq.2019.111707).

30 G. Barbero and I. Lelidis, Fourth-order nematic elasticity and modulated nematic phases: a poor man's approach, *Liq. Cryst.*, 2019, **46**, 535–542, DOI: [10.48550/arXiv.1804.10517](https://doi.org/10.48550/arXiv.1804.10517).

31 M. P. Rossetto and J. V. Selinger, Theory of the splay nematic phase: Single versus double splay, *Phys. Rev. E*, 2020, **101**, 052707, DOI: [10.1103/PhysRevE.101.052707](https://doi.org/10.1103/PhysRevE.101.052707).

32 G. Yu and M. R. Wilson, All-atom simulations of bent liquid crystal dimers: the twist-bend nematic phase and insights into conformational chirality, *Soft Matter*, 2022, **18**, 3087–3096, DOI: [10.1039/D2SM00291D](https://doi.org/10.1039/D2SM00291D).

33 L. Longa, M. Ciesla and A. Chrzanowska, Conformational degrees of freedom and stability of splay-bend ordering in the limit of a very strong planar anchoring, *Phys. Rev. E*, 2023, **107**, 034707, DOI: [10.1103/PhysRevE.107.034707](https://doi.org/10.1103/PhysRevE.107.034707).

34 M. A. Osipov, Theoretical models for the nematic twist-bend phase and the Landau de Gennes theory of Longa and Tomczyk, *Liq. Cryst.*, 2024, **51**, 948–960, DOI: [10.1080/02678292.2024.2321464](https://doi.org/10.1080/02678292.2024.2321464).

35 M. Szmigelski and M. Buczkowska, Structural parameters of twist-bend nematics and splay-bend nematics in Dozov's



theory, *Phys. Rev. E*, 2024, **109**, 044702, DOI: [10.1103/PhysRevE.109.044702](https://doi.org/10.1103/PhysRevE.109.044702).

36 M. Buczkowska, Material parameters ensuring stability of the twist-bend nematic phase, *Liq. Cryst.*, 2024, **51**, 852–856, DOI: [10.1080/02678292.2024.2333318](https://doi.org/10.1080/02678292.2024.2333318).

37 R. J. Mandle and A. Mertelj, Orientational order in the splay nematic ground state, *Phys. Chem. Chem. Phys.*, 2019, **21**, 18769, DOI: [10.1039/c9cp03581h](https://doi.org/10.1039/c9cp03581h).

38 A. Mertelj, L. Cmok and N. Sebastián, *et al.*, Splay Nematic Phase, *Phys. Rev. X*, 2018, **8**, 041025, DOI: [10.1103/PhysRevX.8.041025](https://doi.org/10.1103/PhysRevX.8.041025).

39 F. C. Frank, I. Liquid crystals, On the theory of liquid crystals, *Discuss. Faraday Soc.*, 1958, **25**, 19–28, DOI: [10.1039/DF9582500019](https://doi.org/10.1039/DF9582500019).

40 P. G. de Gennes and J. Prost, *The Physics of Liquid Crystals*, Clarendon Press, Oxford, 1993.

41 M. Kleman and O. D. Lavrentovich, *Soft Matter Physics*, Springer-Verlag, New York, 2003.

42 G. Barbero, L. R. Evangelista and I. Lelidis, A splay-twist nematic phase of bent-shaped mesogens, *Liq. Cryst.*, 2025, DOI: [10.1080/02678292.2025.2470142](https://doi.org/10.1080/02678292.2025.2470142).

43 G. Barbero and L. R. Evangelista, *An Elementary Course on the Continuum Theory for Nematic Liquid Crystals*, World Scientific, Singapore, 2001.

44 S. A. Pikin, *Structural Transformation in Liquid Crystals*, Gordon and Breach Science Publishers, Amsterdam, 1991, p. 181.

45 V. Smirnov, *Cours de mathématiques supérieures*, editions Mir, Moscou 1989, tome IIIa, p. 136.

